

# UPDATE IN THE OPTICS DESIGN OF MONOCHROMATIZATION INTERACTION REGION FOR DIRECT HIGGS $s$ -CHANNEL PRODUCTION AT FCC-ee\*

Z. Zhang<sup>1,2†</sup>, A. Faus-Golfe, CNRS/IN2P3 IJCLab, Université Paris-Saclay, Orsay, France  
 H. Jiang, Elekta Beijing Medical Systems Co. Ltd., Beijing, China  
 B. Bai, Harbin Institute of Technology, Shenzhen, China  
 P. Raimondi, FNAL, Chicago, USA  
 F. Zimmermann, CERN, Geneva, Switzerland  
 K. Oide<sup>3</sup>, University of Geneva, Geneva, Switzerland  
<sup>1</sup>also at Institute of High Energy Physics, Chinese Academy of Sciences, Beijing, China  
<sup>2</sup>also at University of Chinese Academy of Sciences, Beijing, China  
<sup>3</sup>also at KEK, Tsukuba, Japan

## Abstract

The FCC-ee could allow the measurement of the electron Yukawa coupling via direct Higgs  $s$ -channel production at  $\sim 125$  GeV centre-of-mass (CM) energy, provided that the CM energy spread of this channel, can be reduced to about 5–10 MeV to be comparable to the width of the standard model Higgs boson. The natural collision-energy spread at 125 GeV, due only to synchrotron radiation (SR), is about 50 MeV. Its reduction to the desired level can be accomplished by means of “monochromatization”, e.g., through introducing non-zero dispersion of opposite sign at the Interaction Point (IP), for the two colliding beams. This nonzero dispersion at the IP (horizontal or vertical) could be generated by different methods, requiring or not modifications of the Final Focus System (FFS) Local Chromaticity Correction (LCC) system. In this paper we report and compare the different recent Interaction Region (IR) optics design of this new possible collision mode.

## INTRODUCTION

The standard mode of the FCC-ee is designed to operate at four different beam energies of 45.6, 80, 120 and 182.5 GeV, allowing physics precision experiments at the  $Z$ -pole ( $Z$  mode), the  $W$ -pair-threshold (WW mode), the  $ZH$ -maximum ( $ZH$  mode) and above the top-pair-threshold ( $t\bar{t}$  mode) respectively. An optional proposed fifth mode could be the  $s$ -channel Higgs direct production mode. This new proposed collision mode presents an opportunity for the measurement of the electron Yukawa coupling, by directly producing the Higgs at the  $s$ -channel at 125 GeV CM energy, provided that the CM energy spread of this channel, could be reduced to about 5–10 MeV to be comparable to the width of the standard model Higgs boson [1–4]. The natural collision-energy spread at 125 GeV, due only to SR, is about 50 MeV. Reducing it to the desired level can be accomplished by colliding the beams in “monochromatic” mode. This mode of collision, proposed decades ago, consist of establishing inverse correlations between spatial position and energy deviation in the colliding beams [5–16].

\* Work supported by China Scholarship Council (CSC)

† Corresponding author: zhandong.zhang@ijclab.in2p3.fr

In terms of beam optics, this configuration can be achieved by generating a non-zero horizontal or vertical dispersion with opposite signs for the two colliding beams at the IP, so called transverse monochromatization scheme. While lowering the CM energy spread without necessarily decreasing the intrinsic energy spread of the two individual beams, the non-zero dispersion function at the IP will increase the IP transverse beam sizes and could also affect the luminosity. Introducing a monochromatization factor as

$$\lambda = \sqrt{1 + \sigma_\delta^2 \left( \frac{D_x^{*2}}{\varepsilon_x \beta_x^*} + \frac{D_y^{*2}}{\varepsilon_y \beta_y^*} \right)}, \quad (1)$$

the CM energy spread and luminosity of this “monochromatic” mode are both reduced by this factor compared with the standard mode. Therefore, the development of a monochromatization scheme must consider the optimization of other collider parameters to maximize the luminosity while introducing non-zero dispersion at the IP, to achieve a higher rate of Higgs bosons in  $s$ -channel production [17].

Considering the impact of beamstrahlung (BS), a preliminary parametric study of monochromatization for FCC-ee has been made at 125 GeV collision energy prior to the IR beam optics design [18–24]. The FCC-ee monochromatization self-consistent parameters [25] are calculated using Guinea-Pig [15]. Based on these optimized parameters, three different kinds of monochromatization IR optics design are proposed for FCC-ee.

## FCC-ee MONOCHROM IR DESIGN

Two types of FCC-ee standard optics, specifically designed for  $Z$  and  $t\bar{t}$  modes [26, 27], exists. The monochromatization IR optics design has been completed respectively for these two kinds of standard lattice [28]. In the following sections, we will show only the design for the optics based on  $t\bar{t}$  mode lattice. The details of the monochromatization FCC-ee  $t\bar{t}$  mode are summarized in Table 1. For completeness the parameters of the standard  $t\bar{t}$  mode are also included.

### Horizontal Dispersion Generation at the IP

Given the baseline layout of the FCC-ee IR, the nonzero horizontal dispersion at the IP, as required for

monochromatization, can be generated by several sets of different configurations of dipole magnet in the LCC system of FFS [25]. For each set, there are three dipoles composing a chicane structure with three different extra angles which are orderly set manually. The orbit of the monochromatization IR with chicanes is slightly different from the standard orbit. To enhance the flexibility of optics matching, all the IR horizontal dipoles are cut into three pieces and extra thin quadrupoles are inserted between the pieces [29]. After matching and optimizing, we ultimately integrate four smooth close orbit chicanes into the LOC system to create the required horizontal dispersion at the IP while mitigating the horizontal emittance blow up caused by the additional chicane structures [30]. The beam parameters at the IP are matched to be aligned with the FCC-ee monochromatization self-consistent parameters with a horizontal dispersion of 0.105 m [25]. The beam parameters at the entrance and exit of the IR, as well as the phase advances of the LCC sextupoles in the IR are matched to be same as those of the standard optics.

The result of monochromatization IR optics design using MADX [31] is presented in Figure 1. The beam direction is from left to right. Magnetic elements are shown in color (dipoles in blue, quadrupoles in red and sextupoles in green) and the point  $s = 0$  marks the IP. Figure 2 illustrates the comparison between original standard IR orbit (grey) and monochromatization orbit (red), with the point  $Z = 0$  and  $X = 0$  indicating the IP. The position and the angle at the entrance and exit of these two orbits are the same.

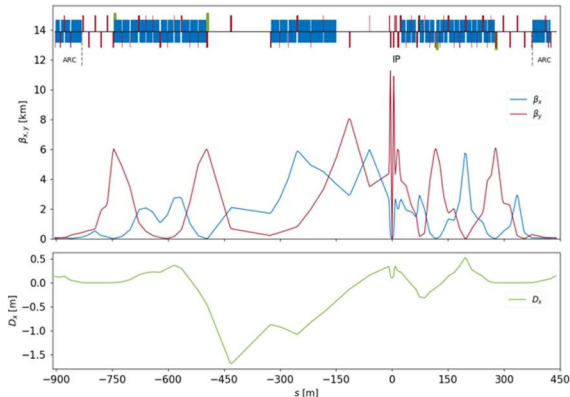


Figure 1: FCC-ee monochromatization IR optics (non-zero horizontal dispersion at the IP).

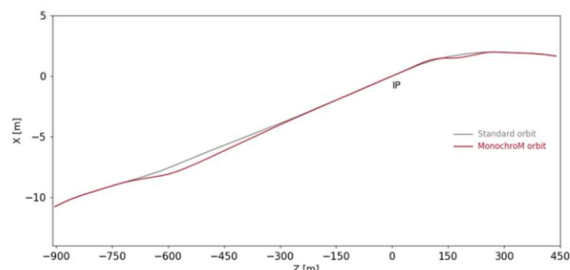


Figure 2: FCC-ee standard IR orbit (grey line) and monochromatization IR orbit (red line).

## Vertical Dispersion Generation at the IP

The FCC-ee, owing to its extremely low vertical emittance (1 pm), features a vertical beam size at the IP much smaller than the horizontal one. Therefore, achieving an adequate monochromatization factor, according to Eq. (1), requires an approximately 100 times smaller vertical dispersion, measuring at 1mm. Introducing this tiny vertical dispersion at the IP can be achieved by adding additional strength in the IR skew quadrupoles, which are needed to correct the skew quadrupole field caused by quadrupole roll errors [32]. These quadrupoles are expected to be implemented at the same locations where the sextupole pairs are installed in the LCC system.

While maintaining a zero vertical dispersion at the entrance and exit of the IR, we match the IP vertical dispersion to 1 mm by varying the strength of the implemented skew quadrupoles. The result is depicted in Figure 3.

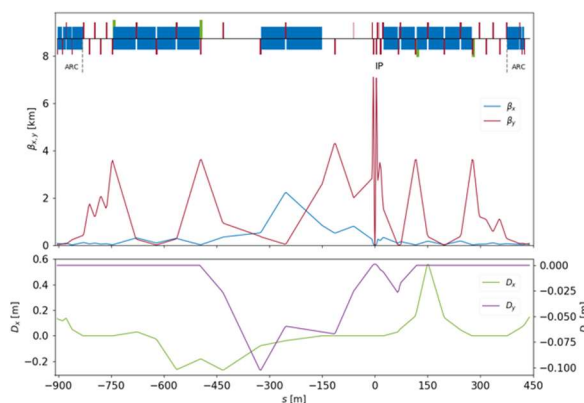


Figure 3: FCC-ee monochromatization IR optics (non-zero vertical dispersion at the IP).

## Mixed Dispersion Generation at the IP

Considering an advantage combination of the two methods mentioned above, we try to implement skew quadrupoles into the monochromatization IR optics with horizontal dispersion at the IP, to introduce mixed dispersion (horizontal dispersion and vertical dispersion) at the IP as shown in Figure 4.

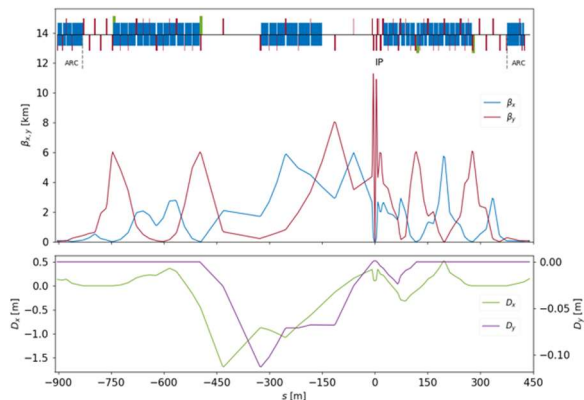


Figure 4: FCC-ee monochromatization IR optics (non-zero mixed dispersion at the IP).

## MONOCHROM IR PERFORMANCE

### Global Implementation

To evaluate the global performance of the three kinds of FCC-ee monochromatization IR optics showed in the previous section, we respectively insert them into the entire ring to replace the original standard IR optics and then, match the global monochromatization ring optics. Before the performance check, we correct the local chromaticity, the global chromaticity and the tune, and we compensate the SR losses [28].

### Luminosity and CM Energy Spread

Using the corrected FCC-ee monochromatization optics, we obtain the parameters without BS computed using the code MADX. Emittance, energy spread and bunch length with the impact of BS are calculated analytically [19]. CM energy spread and luminosity with and without crab cavities are calculated using the code Guinea-Pig. All the performance parameters are summarized in Table 1. The second column in the table presents the parameters of the ttbar mode standard optics operating at 62.5 GeV for comparison. Subsequent columns detail the parameters of the three kinds of FCC-ee monochromatization optics, featuring horizontal dispersion, vertical dispersion and mixed dispersion at the four IPs, respectively.

According to the results presented in Table 1, it is evident that the CM energy spread of the monochromatization mode is significantly decreased compared to the scaled

FCC-ee ttbar mode lattice at 62.5 GeV. Among the three types of monochromatization optics, the configuration with horizontal dispersion at the IP results in higher luminosity but less CM energy spread reduction, whereas the configuration with vertical dispersion at the IP achieves lower CM energy spread but more luminosity loss. The mixed dispersion at the IP combines the advantages of the first two configuration but may potentially face issues related to betatron coupling.

## SUMMARY AND OUTLOOK

Three distinct monochromatization IR optics have been implemented for FCC-ee, each incorporating the necessary dispersion at the IPs. A preliminary global performance comparison of these novel IR optics design has been completed, with a specific emphasis on their CM energy spread and luminosity. The dynamic aperture optimization and beam-beam studies are still in progress. Future plans involve initiating monochromatization investigations at Circular Electron Positron Collider (CEPC) and experimental proof of monochromatization concept in running e<sup>+</sup>e<sup>-</sup> low energy colliders.

## ACKNOWLEDGEMENTS

We would like to thank A. Blondel, P. Janot, D. d'Enterria, D. Shatilov, J. Keintzel, G. Wilkinson and J. Wenninger for fruitful discussions in the EPOL FCC-ee working group.

Table 1: Performance Parameters of FCC-ee Standard Optics and Monochromatization Optics

Parameters		Standard	Standard Scaled*	MonochroM Horizontal	MonochroM Vertical	MonochroM Mixed
# of IPs $n_{IP}$	[ / ]			4		
Circumference	[m]			91174.117		
Beam energy $E$	[GeV]	182.5	62.5	62.5	62.5	62.5
Energy loss/turn	[MeV]	10000.0	137.6	143.5	137.6	143.4
SR power loss	[MW]	50	54.3	56.7	54.3	56.7
Beam current $I_e$	[mA]	5	395	395	395	395
Bunches/beam $n_b$	[ / ]	40	13420	13420	13420	13420
Bunch population $N_b$	[10 <sup>11</sup> ]	2.37	0.56	0.56	0.56	0.56
Horizontal emittance $\epsilon_x$ (SR/BS)	[nm]	1.49/1.49	0.17/0.17	1.48/4.31	0.17/0.17	1.48/4.31
Vertical emittance $\epsilon_y$	[pm]	2.98	0.34	2.96	0.35	2.96
Momentum compaction factor $\alpha_c$	[10 <sup>-6</sup> ]	6.99	7.30	6.92	7.31	6.92
$\beta_{x/y}^*$	[mm]	1000/1.6	1000/1.6	90/1	1000/1.6	90/1
$D_{x/y}^*$	[m]	0/0	0/0	0.105/0	0/0.001	0.105/0.001
Energy spread $\sigma_\delta$ (SR/BS)	[%]	0.16/0.22	0.05/0.09	0.06/0.06	0.05/0.09	0.06/0.06
Bunch length $\sigma_z$ (SR/BS)	[mm]	2.03/2.70	3.86/6.18	4.05/4.13	3.86/6.18	4.05/4.13
Synchrotron tune $Q_s$	[ / ]	0.082	0.015	0.014	0.015	0.014
Longitudinal damping time	[turns]	18.5	454	436	454	436
CM energy spread $\sigma_W$ (w/o crab cavity)	[MeV]	547/542	75.9/76.7	15.9/25.9	9.10/4.94	7.64/6.36
Luminosity (w/o crab cavity)	[10 <sup>34</sup> cm <sup>-2</sup> s <sup>-1</sup> ]	1.83/1.52	399/122	33.7/29.4	21.2/2.98	14.8/6.43

\* No realistic implementation, only energy scaled.

## REFERENCES

- [1] M. Mangano (ed.) *et al.*, “FCC physics opportunities”, *Eur. Phys. J. C*, vol. 79, no. 6, p. 474, Jun. 2019. doi:10.1140/epjc/s10052-019-6904-3
- [2] A. Abada *et al.*, “FCC-ee: the lepton collider”, *Eur. Phys. J. Spec. Top.*, vol. 228, pp. 261-623, Jun. 2019. doi:10.1140/epjst/e2019-900045-4
- [3] S. Jadach, R. A. Kycia, “Lineshape of the Higgs boson in future lepton colliders”, *Phys. Lett. B*, vol. 755, pp. 58–63, Apr. 2016. doi:10.1016/j.physletb.2016.01.065
- [4] H. Jiang, A. Faus-Golfe, F. Zimmermann, K. Oide, “Update on the monochromatization studies”, in *Proc. FCC-FS EPOL group and FCCIS WP2.5 meeting 4*, Jan. 2022.
- [5] A. Renieri, “Possibility of achieving very high-energy resolution in electron-positron storage rings”, Rep. LNF-75/6-R, Feb. 1975.
- [6] M. Bassetti *et al.*, “ADONE: present status and experiments”, Stanford, CA, USA, Rep. LNF-74-22-P, May. 1974.
- [7] I. Y. Protopopov, A. N. Skrinsky, A. A. Zholents, “Energy monochromatization of particle interaction in storage rings”, Rep. IYF-79-06, Jan. 1979.
- [8] A. A. Avdienko *et al.*, “The project of modernization of the VEPP-4 storage ring for monochromatic experiments in the energy range of psi and upsilon mesons”, in *Proc. HEACC'83*, Batavia, Aug. 1983, pp. 186-189.
- [9] Y. I. Alexahin, A. N. Dubrovin, A. A. Zholents, “Proposal on a tau charm factory with monochromatization”, in *Proc. EPAC'90*, Nice, France, Jun. 1990, pp. 398-401.
- [10] A. A. Zholents, “Polarized J/psi mesons at a tau charm factory with a monochromator scheme”, CERN, Geneva, Switzerland, Rep. CERN-SL-92-27-AP, Jun. 1992.
- [11] A. Faus-Golfe, J. Le Duff, “Versatile DBA and TBA lattices for a tau charm factory with and without beam monochromatization”, *Nucl. Instrum. Methods Phys. Res., Sect. A*, vol. 372, pp. 6-18, Mar. 1996. doi:10.1016/0168-9002(95)01275-3
- [12] A. A. Zholents, “Sophisticated accelerator techniques for colliding beam experiments”, *Nucl. Instrum. Methods Phys. Res., Sect. A*, vol. 265, pp. 179-185, Mar. 1988. doi:10.1016/0168-9002(88)91070-4
- [13] K. Wille, A. W. Chao, “Investigation of a monochromator scheme for SPEAR”, Rep. SLAC/AP-032, Aug. 1984.
- [14] M. Bassetti, J. M. Jowett, “Improving the energy resolution of LEP experiments”, Washington, D.C., Rep. CERN-LEP-TH-87-09, Mar. 1987.
- [15] D. Schulte, “Study of electromagnetic and hadronic background in the interaction region of the TESLA collider”, Ph.D. thesis, U. Hamburg, Germany, 1997.
- [16] J. M. Jowett, “Feasibility of a monochromator scheme in LEP”, CERN, Geneva, Switzerland, Rep. CERN-LEP-Note-544, Sep. 1985.
- [17] D. d'Enterria *et al.*, “Measuring the electron Yukawa coupling via resonant s-channel Higgs production at FCC-ee”, *Eur. Phys. J. Plus*, vol. 137, no. 2, p. 201, Feb. 2022. doi:10.1140/epjp/s13360-021-02204-2
- [18] M. A. Valdivia García, A. Faus-Golfe, F. Zimmermann, “Towards a monochromatization scheme for direct Higgs production at FCC-ee”, in *Proc. IPAC'16*, Busan, Korea, May. 2016, pp. 2434-2437. doi:10.18429/JACoW-IPAC2016-WPEMW009
- [19] M. A. Valdivia García, F. Zimmermann, “Towards an optimized monochromatization for direct Higgs production in future circular e+ e- Colliders”, in *CERN Proc.*, vol. 1, pp. 1-12. doi:10.23727/CERN-Proceedings-2017-001.1
- [20] A. Bogomyagkov, E. Levichev, “Collision monochromatization in e+e- colliders”, *Phys. Rev. Accel. Beams*, vol. 20, no. 5, p. 051001, May 2017. (Erratum: *Phys. Rev. Accel. Beams*, vol. 21, p. 029902, 2017). doi:10.1103/PhysRevAccelBeams.20.051001
- [21] V. I. Telnov, “Monochromatization of e+e- colliders with a large crossing angle”, Sep. 2020. arXiv:2008.13668
- [22] F. Zimmermann, M. A. Valdivia García, “Optimized monochromatization for direct Higgs production in future circular e+e- colliders”, in *Proc. IPAC'17*, Copenhagen, Denmark, May. 2017, pp. 2950-2953. doi:10.18429/JACoW-IPAC2017-WEPIK015
- [23] M. A. Valdivia García, F. Zimmermann, “Effect of emittance constraints on monochromatization at the Future Circular e+e- Collider”, in *Proc. IPAC'19*, Melbourne, Australia, May 2019, pp. 516-519. doi:10.18429/JACoW-IPAC2019-MOPMP035
- [24] M. A. Valdivia Garcia, F. Zimmermann, “Beam blow up due to beamstrahlung in circular e+e- Colliders”, *Eur. Phys. J. Plus*, vol. 136, no. 5, pp. 1-18, May 2021. doi:10.1140/epjp/s13360-021-01485-x
- [25] A. Faus-Golfe, M. A. Valdivia Garcia, F. Zimmermann, “The challenge of monochromatization: direct s-channel Higgs production: e+e- → H”, *Eur. Phys. J. Plus*, vol. 137, no. 1, p. 31, Dec. 2021. doi:10.1140/epjp/s13360-021-02151-y
- [26] J. Keintzel *et al.*, “FCC-ee lattice design”, in *JACoW eeFACT 2022*, pp. 52-60. doi:10.18429/JACoW-eeFACT2022-TUYAT0102
- [27] K. Oide *et al.*, “Design of beam optics for the future circular collider e+e- collider rings”, *Phys. Rev. Accel. Beams*, vol. 19, p. 1111005, Nov. 2016. (Erratum *Phys. Rev. Accel. Beams*, vol. 20, p. 049901, 2017). doi:10.1103/PhysRevAccelBeams.19.111005
- [28] Z. Zhang *et al.*, “Monochromatization optics design for FCC-ee”, in *Proc. CEPC EU Workshop 2024*, Marseille, France, Apr. 2024.
- [29] Z. Zhang *et al.*, “Monochromatization interaction region optics design for direct s-channel production at FCC-ee”, in *Proc. IPAC'23*, Venice, Italy, May. 2023, pp. 738-741. doi:10.18429/JACoW-IPAC2023-MOPL079
- [30] Z. Zhang *et al.*, “Monochromatization optics for FCC-ee lattices”, in *Proc. CEPC Workshop 2023*, Nanjing, China, Oct. 2023.
- [31] MADX - Methodical Accelerator Design. <http://madx.web.cern.ch/madx/>
- [32] T. K. Charles *et al.*, “Alignment & stability challenges for FCC-ee”, *EPJ Tech. Instrum.*, vol. 10, no. 1, p. 8, Mar. 2023. doi:10.1140/epjti/s40485-023-00096-3